JOINT CONTROL OF COMMUNICATION SUBSYSTEMS FOR LOW-ENERGY IMAGE TRANSMISSION

Hunsoo Choo and Kaushik Roy

Low Power VLSI Lab, Electrical & Computer Engineering
Purdue University, West Lafayette, IN 47907
E-mail:chooh,kaushik@ecn.purdue.edu.

ABSTRACT

This paper presents a joint control method for low-energy image transmission. The proposed method is based on *universal distortion-rate characteristics*, which are pre-determined characteristics of a source coder. This method relieves the computational cost of the joint optimization involving source coder, channel coder and modulation by separating source coder and other communication subsystems. The results show that an average of 23% energy saving over reference system can be achieved when targeting mid-quality of image ($33dB$ PSNR) under fading channel when fading figure is 3.

1. INTRODUCTION

Wireless communication market is expanding rapidly along with the growing demand for robust and efficient services of voice, data, image and video transmission over wireless communication channel. Among them, image and video transmissions are especially challenging due to increased computation, bandwidth efficiency and transmission speed requirements as well as the time varying characteristic of the communication channel. On the other hand, integrating more and more components in a single device and powering them by limited energy source like battery have become an important issue in wireless communication.

Recently, micro-cells have become the center of interest for near-distance (1∼100m) communication. In this communication range, transmission energy is not a dominant factor in total communication energy [10, 11]. The baseband processing units and the analog front-end circuitry contribute a substantial portion of the total dissipated energy. In [1, 2], authors tried to optimize energy cost to communicate a signal between transmitter and the receiver. They considered the energy dissipations of channel coder and analog/RF circuitry. Modulation scaling was introduced in [3, 4, 5] and the effects of different modulation schemes on communication energy were investigated considering total transmission time. In [6, 7], authors specifically considered image and video transmission and introduce joint source and channel optimization methods to minimize communication energy. They focused mainly on source coding and channel coding rates to trade-off energy and image quality. The above techniques were to achieve the desired quality of service (QoS) using the right amount of energy. It can be easily imagined that an optimization technique simultaneously considering adaptive modulation and souce/channel coding, can further minimize the total energy. However, it is difficult to consider modulation and source/channel code rates altogether, because it increases computational complexity significantly. Hence, there is a need for a simpler method for optimizing the communication energy.

This research was supported in part by Semiconductor Research Corporation.

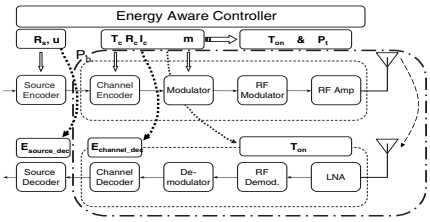

Fig. 1. Energy-aware image transmission

In this paper, we propose a joint optimization method considering source coder, channel coder and modulator to minimum energy consumption in image transmission. The proposed method is based on *universal distortion-rate characteristics* (UDRC) which are the characteristics of each source coder [8]. It is shown that source coder and other communication blocks can be considered separately due to the feature of UDRC and optimized system configurations can be obtained with lower complexity.

2. WIRELESS LINK

Traditionally, communication systems are designed for worst channel conditions. Though these approaches provide robust services, usually they sacrifice energy efficiency. Multimedia systems require large DSP components which are very computationally intensive. Energy dissipation in digital processing block and analog circuitry contributes a substantial portion of the total energy consumption. Generally, transmission power is determined by SNR (signal to noise ratio) requirement of arriving signal at the receiver. The SNR requirement can be varied by changing the error correction capability and the channel error sensitivity of source coded image. This in turn, affect the energy cost of digital processing blocks. Hence, total communication energy can be reduced by properly controlling the error sensitivity of signal and the transmission power.

An energy controllable communication system can be obtained by implementing reconfigurable source/channel coder and modulator where power performance trade-offs can be made. Figure 1 shows a diagram of multimedia system. The wireless system dynamically selects the configuration of each subsystem based on multimedia quality requirement and the channel condition. Energy aware controller plays the role of a system manager to control each subsystem for high energy efficiency.

It is assumed that channel coder can be reconfigured to Viterbi and turbo coder (T_c: coder type) with several different code rates (R_c) and iteration number (I_c for turbo). We also assume that

modulation order (m) and compression rate (R_s) of source coder can be reconfigured by the system controller. These enable us to exploit the trade-offs between the transmission energy and the circuit processing energy. We investigate the impact of communication subsystems on total communication energy by focusing on the following subsystems: source coder, channel coder, modulator, analog circuitry and the RF amplifier. For simplicity of analysis, perfect channel feedback is assumed and complex issues in analog circuit implementation for higher order modulation are ignored.

The objective is to minimize the energy cost to transmit an image under quality constraints. The total communication energy cost per pixel, ε_{pixel} has two components: digital processing energy (ε^d) and analog/RF processing energy (ε^a_{total}). ε^d has two components which are the energy consumption in source coder (ε_s) and the energy consumption in channel coder (ε_c). Since, ε_s is a function of (R_s), ε_c is a function of (T_c, R_c, I_c) and ε^a_{total} is determined by (R_s, R_c, T_c, I_c, m), system configuration parameters, (R_s, T_c, R_c, I_c, m) determine ε_{pixel}. The energy minimization problem then can be expressed as

$$\text{argmin}_{(R_s,T_c,I_c,R_c,m)}\ \varepsilon_{pixel} \qquad \text{s.t. } Q_r > Q_c \tag{1}$$

where Q_r and Q_c represent the image quality at the receiver and minimum image quality constraint, respectively. Q_r is determined by errors occurred in source coder and the communication channel, which are also affected by (R_s, T_c, R_c, I_c, m).

In conventional joint source and channel coding with fixed modulation scheme, the image distortion caused by errors is determined by joint code rate $R_{s+c} = R_s/R_c$ and the optimization of Q_r is performed based on the *rate-distortion curve* (RDC). However, as the number of system parameters affecting the channel error increases, the complexity of this method increases dramatically, since RDC needs to be re-calculated on all pairs of system parameters. We also consider T_c, I_c and m as system parameters and hence, it is not preferred to use conventional method.

Figure 2(a) shows example plots of *universal distortion-rate characteristics* (UDRC), which were introduced in [8]. These characteristic curves are obtained considering P_b (bit error rate) and R_s instead of R_{s+c}. Here, P_b is an accumulated statistical error affecting the channel without considering any particular factor. Hence, UDRC shows the inherent characteristic of a source coder and it does not have to be re-calculated though any parameter (T_c, R_c, I_c, m) or channel condition is changed. It is therefore, possible to consider source coder and other subsystems separately for overall energy optimization reducing the computational complexity. P_b is a parameter which interlocks source coder and other subsystems.

It was presented that system configurations for channel coder and modulation to minimize communication energy, can be obtained under BER constraint without considering the source coder [10]. Similar approach can be applied to multimedia transmission by using UDRC of source coder without significantly increasing the computational complexity.

ε_{pixel} can be expressed as

$$\varepsilon_{pixel} = \frac{\varepsilon_s}{WH} + b \cdot R_s \cdot \frac{\varepsilon_c(\tau, R_c, I_c, T_c) + \varepsilon^a_{total}(R_c, m, \gamma)}{K} \tag{2}$$

where K is the frame length for channel coder, $b \cdot R_s$ is the number of bit per pixel and b is the bit length for a pixel. W and H are the width and height of the image, respectively. ε_c and ε^a_{total} are energy dissipations to process K bits of incoming sinal to channel coder. Hence, $(\varepsilon_c + \varepsilon^a_{total})/K$ represents the energy dissipation to transmit one bit (ε_{bit}).

The optimization of communication energy is performed as follows:

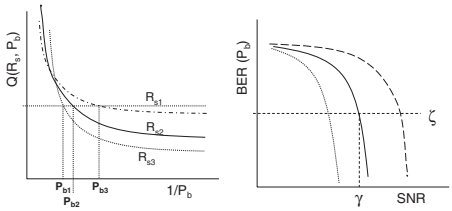

(a) UDRC (b) BER curve

Fig. 2. Minimization based on UDRC

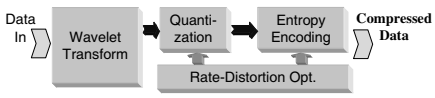

Fig. 3. Diagram for wavelet-based image compression

	Analysis Filter Coefficients	Complexity
LP	$\frac{-x[2n-2]+2x[2n-1]+6x[2n]+2x[2n+1]-x[2n+2]}{8}$	8 SH+3 A+2 S
HP	$\frac{x[2n]-2x[2n+1]+x[2n+2]}{2}$	2SH+1 A+ S
	Synthesis Filter Coefficients	**Complexity**
LP	$\frac{x[2n]+2x[2n+1]+x[2n+2]}{2}$	2 SH+2 A
HP	$\frac{x[2n-2]+2x[2n-1]-6x[2n]+2x[2n+1]+x[2n+2]}{8}$	8 SH+4 A+S

• SH: shift operation, A: addition, S: subtraction

Table 1. Coefficients of 5/3 wavelet filters

For a given Q_c, possible pairs of (P_b, R_s) are obtained from UDRC (Figure 2(a)). For each pair of (P_b, R_s), the channel configuration (T_c, R_c, I_c, m) and SNR requirement which minimize ε_{bit} under BER constraint (ξ) is determined (Figure 2(b)). Finally, the optimized configuration set is determined by comparing ε_{pixel} of all configurations.

The energy and performance model of each subsystem are described in the following section.

3. SYSTEM PERFORMANCE

3.1. Performance of Source Coder

Figure 3 shows the block diagram of source coder. Image compression is performed based on wavelet transformation implemented using an energy reconfigurable technique called *H* elimination* [12]. Table 1 shows $5/3$ taps filters which are used for wavelet transformation. 2D wavelet transformation (WT) divides the image into four frequency bands (LL, LH, HL and HH). In most cases, LL band is considered to include large values, while other bands include small values. In H* elimination, all data including high frequency component are ignored from further processing (Figure 4(a)) to reduce energy cost. For example, let us assume 2D WT is applied l times. Then, the image will be divided into several frequency bands which are similar to Figure 4(a) where $l = 3$. If LH, HL and HH of level 1 are decided not to be used, only LL_1 is computed and u, the smallest level index which is used for transformation, is set to 2.

Performance of source coder is tested after quantizer, arithmetic coder and simple distortion-rate optimization block are added. Figure 4(b) shows example characteristic graphs of H* elimination when $(l, u) = (6, 2)$. From our simulation, three pairs of (l, u), $\{(6,1), (6,2), (6,3)\}$ show reasonable performance enough to reconstruct an image with $29dB$ PSNR.

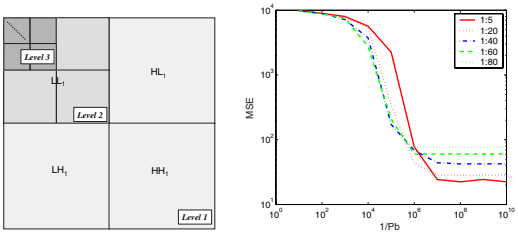

(a) Wavelet domain (b) (l,u) = (6,2)

Fig. 4. Wavelet Transformation

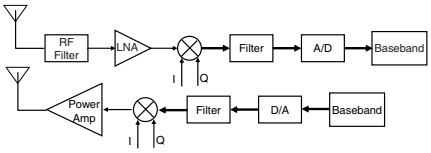

Fig. 5. Transceiver architecture

3.2. Performance of Convolutionary Coded MQAM

It is well known that the symbol error rate of MQAM under Nakagami fading channel is represented as [9]

$$\zeta_s^M = 4q[\tfrac{1}{2}(1-\hat{\lambda})]^{f_d}\sum_{k=0}^{f_d-1}\binom{f_d-1+k}{k}[\tfrac{1}{2}(1+\hat{\lambda})]^k - \frac{q^2\lambda^{f_d}(-1)^{f_d-1}}{(f_d-1)!}\{\frac{d^{f_d-1}}{ds^{f_d-1}}[\frac{1}{s}-\frac{4}{\pi}\frac{tan^{-1}(\varrho)}{s\cdot\varrho}]|_{s=\lambda}\} \quad (3)$$

where $\hat{\lambda}=\sqrt{\frac{p}{p+\lambda}}$, $\varrho=\sqrt{1+\frac{s}{p}}$, f_d is fading figure, γ is average received SNR. $\lambda=\frac{f_d}{\gamma}$ and $p=\frac{3}{2}log_2\frac{M}{M-1}$ and $q=1-\frac{1}{\sqrt{M}}$ ($M=2^m$). The BER can be obtained by dividing ζ_s^M by $\sqrt{M}$. In our simulation, m is selected from $\{2,4,6,8,10\}$.

It is hard to formulate the performance of Viterbi or turbo decoder in a closed form as a function of (R_s,m). Hence, the performances of two convolutional decoders are estimated by coding gain which is independent of the modulation scheme. A Viterbi coder [13] and a parallely concatenated turbo coder [14] are implemented in C program with finite precision. Their coding gains are obtained from simulation for different code rates and iteration numbers. Code rate of Viterbi decoder is $\{\frac{3}{4},\frac{2}{3},\frac{1}{2},\frac{1}{3},\frac{1}{4},\frac{1}{5}\}$ and code rate of turbo decoder is $\{\frac{4}{5},\frac{3}{4},\frac{2}{3},\frac{1}{2},\frac{1}{3},\frac{1}{4},\frac{1}{5}\}$. Maximum iteration of turbo coder is limited to 8.

4. ENERGY MODEL

[Digital Processing] The source/channel coder consists of memory and basic arithmetic computation logic like adder, subtractor and ACS. Complexities of source/channel coder are calculated based on the total number of basic computations and memory access frequency. Table 2 summarizes the estimated energy models based on the equations which are introduced in [13, 14]. $\varepsilon_s(=\varepsilon_{s:enc}+\varepsilon_{s:dec})$ is the total energy consumption of source coder to encode and decode an image with W (width) and H (height). ε_c is the energy dissipation of channel decoder to decode K bits.

The energy estimation of basic blocks like adder, subtractor, ACS, VM (vector multiplication for Viterbi decoder), memory etc. is summarized in Table 3 and 4. These data are obtained from HSPICE simulation using netlists obtained from layouts. On the other hand, energy dissipation of each memory access is estimated using *Cacti* simulator [15]. TSMC .25μm technology with 2.5V nominal supply voltage is assumed and 8bit wordlength is used for all internal values of source/channel coder.

	E_{ADD}	E_{SUB}	E_{ACS}	$E_{MULT\pm1}$	E_{VM}
Unit [uJ]	2.7	2.7	14.7	5	11.1

Table 3. Energy dissipation in basic arithmetic blocks

	Memory Size	Constraint Length	Energy [nJ]
Image coding	$W \cdot H$ bytes		4.09
Viterbi (PMU)	$(K+\tau)\cdot\Gamma^2\cdot w$	7	7.29
		5	1.3
		3	0.87
Turbo (BMU)	$2K\cdot\Gamma\cdot w$	5	1.3
Turbo (FMU)	$2K\cdot\Gamma\cdot w$	5	1.06

* w is wordlength, K is frame length for decoder, τ is constraint length
Γ is total number of states in trellis

Table 4. Energy dissipation per memory access

[Analog Front-End/RF] Figure 5 shows a simple diagram of low-IF transceiver. Effects of ADC and DAC are ignored for simplicity. Energy dissipation of analog front-end and RF amplifier can be expressed as [10]

$$\varepsilon_{total}^a = (P_{tr}^c + P_{rec}^c + \frac{P_t}{\eta(P_t)})\cdot T_{on} \quad (4)$$

Where P_{tr}^c and P_{rec}^c are the power dissipations of analog circuitry (filters, mixer, LNA, frequency synthesizer etc.) in transmitter and the receiver, respectively. P_t is RF transmit power and $\eta(P_t)$ is the power aided efficiency (PAE) which is calculated as $\eta_{max}\sqrt{P_t/P_{t,max}}$. First-order approximation allows us to estimate P_{tr}^c and P_{rec}^c as $82.5mW$ and $106.1mW$, respectively [4].

Transmitted signal suffers from propagation loss and fading effect over the communication channel. P_t is calculated following equation (5) where γ is the required SNR at the receiver to meet the BER constraint [10]

$$P_t \approx (2B\cdot No)\cdot NF\cdot\gamma\cdot M_l\cdot(4\pi)^3\cdot d^3 \quad (5)$$

where B is bandwidth for modulated symbol and NF is noise figure. For our simulation, $\eta_{max}=50\%$, $P_{t,max}=100mW$, $No=-174dBm/Hz$, $B=100KHz$ and $NF=10dB$. An additional link margin(M_l) of $35dB$ is also considered. Finally, energy dissipation per bit in analog and RF circuitry can be expressed as

$$\varepsilon_{total}^a/bit = \frac{\varepsilon_{total}^a}{K} = \frac{(P_{tr}^c + P_{rec}^c + \frac{\sqrt{P_{t,max}}}{\eta_{max}}\cdot\sqrt{\mu B\gamma d^3})}{B\cdot R_c\cdot m} \quad (6)$$

where $\mu=2\cdot No\cdot NF\cdot M_l\cdot(4\pi)^3$ and $T_{on}=\frac{1}{B}\cdot\frac{K}{R_c\cdot m}$.

5. RESULTS

The proposed communication system is simulated for various communication distances with a range from 5m to 200m. m is considered to be $\{2,4,6,8,10\}$. Code rates for viterbi and turbo coders are $\{\frac{3}{4},\frac{2}{3},\frac{1}{2},\frac{1}{3},\frac{1}{4},\frac{1}{5}\}$ and $\{\frac{4}{5},\frac{3}{4},\frac{2}{3},\frac{1}{2},\frac{1}{3},\frac{1}{4},\frac{1}{5}\}$ respectively. Maximum iteration of turbo decoder is limited to 8. Regarding source coder, R_s is assumed to be between 1:1 and 1:60. Various channel conditions are considered by changing fading figures (1 (rayleigh), 3, and 6). UDRC of source coder is calculated statistically for each pair of (l,u), $\{(l,u)|(6,1),(6,2),(6,3)\}$, by testing with 512 $\times$ 512 Lena image 100 times. Q_c is set to 29 or 33dB in PSNR.

Figure 6 shows the comparison between minimum energy and energy of fixed systems. Fixed systems are assumed to have $(l,u)=(6,1)$, $m=2$ and $R_c=1/2$(Viterbi),1/3(turbo, 6 maximum iterations). However, R_s is assumed to be optimally selected in terms of energy. In case of $f_d=3$ and $Q_c=33dB$, 23% energy saving is obtained over reference system on average. When targeting $29dB$ PSNR, energy can be saved by 18% over reference system on average. The reference system is assumed to be able to

Source coder	Encode $\varepsilon_{s:enc}$	$HW\Big\{\ 1-(\frac{1}{4})^{u-1}\ \ (8E_{SHIFT}+3E_{ADD}+2E_{SUB}+2E_{mread}+E_{mwrite})+$ $\frac{8}{3}(\frac{1}{4})^{u-1}\cdot(1-4^{-l})(E_{mread}+E_{mwrite})+\frac{4}{3}\ \ (\frac{1}{4})^{u-1}-(\frac{1}{4})^{l}\ \ (10E_{SHIFT}+4E_{ADD}+3E_{SUB})\Big\}$
	Decode $\varepsilon_{s:dec}$	$HW\Big\{\ 1-(\frac{1}{4})^{u-1}\ \ (2E_{SHIFT}+2E_{ADD}+E_{mread}+2E_{mwrite})+$ $\frac{8}{3}(\frac{1}{4})^{u-1}\cdot(1-4^{-l})(E_{mread}+E_{mwrite})+\frac{4}{3}\ \ (\frac{1}{4})^{u-1}-(\frac{1}{4})^{l}\ \ (10E_{SHIFT}+6E_{ADD}+E_{SUB})\Big\}$
Viterbi decoder		$(K+\tau)\{2^{n}(n-1)\cdot E_{ADD}+E_{ACS}\cdot\Gamma\}+K(\Gamma+1)\cdot(E_{VM}+2\cdot E_{mread}+E_{mwrite})$
Turbo decoder		$(K+\tau)\{2\Gamma\cdot E_{ADD}+2\Gamma\cdot(n+1)\cdot E_{MULT^{\pm1}}+4\Gamma\cdot E_{ACS}+E_{SUB}+2(\Gamma-1)\cdot E_{MAX}\}$ $+K\Gamma(3E_{mwrite}+6E_{mwrite})$

• K: frame length of channel decoder, τ: constraint length, Γ: total number of states in trellis • $MULT^{\pm1}$: multiplication with ±1, E_{SHIFT} is assumed to be zero

Table 2. Energy models of digital baseband blocks

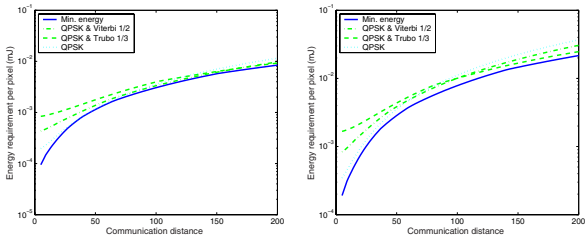

(a) $Q_c = 29dB$ (b) $Q_c = 33dB$

Fig. 6. Total energy ($f_d = 3$)

reconfigure itself to optimally uncoded system and Viterbi coder ($R_c = 1/2$) with QPSK.

Especially when targeting low quality of image ($29dB$), even though $(l, u) = (6, 3)$ can achieve $29dB$ PSNR with lowest $\varepsilon_s/pixel$, it is proved that it does not guarantee minimum energy cost for a short communication distance. It is due to degraded channel sensitivity. It is shown in Figure 7(a) which describes best configuration of source coder depending on communication distance. In addition, Figure 7(b) shows efficient channel coder at each communication distance under rayleigh channel. It is found that turbo coder can be useful for energy efficiency despite its own high complexity when channel condition is not good. The coding gain of turbo decoder is preferred to be controlled by I_c rather than R_c. In addition, high code rate proves to be energy efficient rather than low code rate which has strong coding gain. This shows that energy efficient design need to have different reconfigurable features.

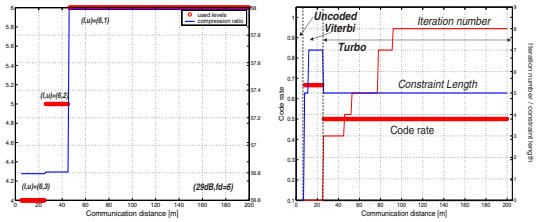

(a) Source coder (b) Channel coder (Q_c=33dB,Rayleigh)

Fig. 7. System configuration

6. CONCLUSION

A joint control method with reduced complexity is presented to minimize the energy cost. The suggested method is based on universal distortion-rate characteristics. Source/channel coder and modulation schemes can be optimized jointly without increasing computational complexity by separating source coder from other subsystems. On average 23% energy saving is obtained over reference system when targeting 33dB PSNR of image distortion.

7. REFERENCES

[1] R. Min, el al., "Energy-centric enabling technologies for wireless sensor networks," in *IEEE Wireless Communications*, Aug 2002, vol. 9, pp. 28–39.

[2] W. E. Stark, el al., "Low-energy wireless communication network design," in *IEEE Wireless Communications*, Aug 2002, vol. 9, pp. 60–72.

[3] C. Schurgers, el al., "Modulation scaling for energy aware communication systems," in *ISLPED*, Aug 2001, pp. 96–9.

[4] S. Cui, el al., "Modulation optimization under energy constraints," in *IEEE ICC*, 2003, vol. 4, pp. 2805–11.

[5] A. Y. Wang, el al., "Energy efficient modulation and mac for asymmetric RF microsensor systems," in *ISLPED*, Aug 2001, pp. 106–11.

[6] Z. Ji, el al., "End-to-end power-optimized video communication over wireless channels," in *IEEE MMSP*, Oct 2001, pp. 447–52.

[7] M. Goel, el al., "A low-power multimedia communication system for indoor wireless applications," in *IEEE SiPS 99*, Oct 1999, pp. 473–82.

[8] M. Bystrom and J.W. Modestino, "Combined source-channel coding schemes for video transmission over an additive white gaussian noise channel," *IEEE Journal on Selected Areas in Communications*, vol. 18, pp. 880–90, 2000.

[9] A. Annamalai, el al., "Exact evaluation of maximal-ratio and equal-gain diversity receivers for M-ary QAM on nakagami fading channels," *IEEE Trans. on Communications*, vol. 47, no. 9, pp. 1335–44, Sept 1999.

[10] H. Choo and K. Roy, "Parametric approach for low energy wireless data communication," in *To appear in 2004 IEEE SiPS*, Oct 2004.

[11] R. Min and A. P. Chandrakasan, "A framework for energy-scalable communication in high-density wireless networks," in *ISLPED*, 2002, pp. 36–41.

[12] D.-G. Lee and S. Dey, "Adaptive and energy efficient wavelet image compression for mobile multimedia data services," in *IEEE ICC 2002*, 28 Apr-2 May 2002, vol. 4, pp. 2484–90.

[13] G. Fettweis, "Algebraic survival memory management design for Viterbi detectors," *IEEE Trans. on Communications*, vol. 43, no. 9, pp. 2458–63, Sep 1995.

[14] P. Jung and M. M. Naβhan, "Comprehensive comparison of turbo-code decoders," in *IEEE 45th VTC1995*, July 1995, vol. 2, pp. 624–8.

[15] S.J.E. Wilton and N.P. Jouppi, "Cacti: an enhanced cache access and cycle time model," *IEEE Journal of Solid-State Circuits*, vol. 31, pp. 677–88, Sep 1996.